NANO-MICRO LETTERS ARTICLE
www.nmletters.org

Synthesis and Characterization of CaF_2 Nanoparticles with Different Doping Concentrations of Er^{3+}

Jinghong Song, Guanglin Zhi*, Yan Zhang, Bingchu Mei

(Received 20 April 2011; accepted 17 June 2011 published online 23 June 2011.)

Abstract: Calcium fluoride nanoparticles with various amounts of erbium ion dopants were prepared by CTAB/C_4H_9OH/C_7H_{16}/H_2O reverse micro-emulsion method. The nanoparticles were studied by X-ray diffraction (XRD), transmission electron microscopy (TEM), fourier transform infrared spectroscopy (FTIR), absorption and fluorescence spectra. The XRD patterns indicate a typical cubic fluorite structure and no other impurities. TEM results show the synthesized particles having uniform grain size and without agglomeration. FTIR spectra reveal that there are some amounts of -OH, NO_3^- and other organic functional groups on the particle surfaces before the annealing process. Many absorption peaks and bands are present in the absorption spectra, corresponding to the rich energy levels of erbium ion. The Red-Shift of absorption bands and Blue-Shift of fluorescence peaks can be attributed to the weakened energy level split as a result of the decrease in crystal field strength.
Keywords: CaF_2; Nanoparticles; Doping; Erbium ions

Citation: Jinghong Song, Guanglin Zhi, Yan Zhang and Bingchu Mei, "Synthesis and Characterization of CaF_2 Nanoparticles with Different Doping Concentrations of Er^{3+}", Nano-Micro Lett. 3 (2), 73-78 (2011). http://dx.doi.org/10.3786/nml.v3i2.p73-78

Introduction

As one of the traditional optical materials, calcium fluoride exhibits a series of advantages compared with oxide compounds, including lower phonon energy [1], melting point, and refractive index [2], as well as the higher optical transmittance and broader transmittance range [2]. Moreover, the typical fluorite structure of calcium fluoride enables high doping concentration of foreign ions. Thus, on the one hand, calcium fluoride with high purity is applied in the fields such as ultraviolet lithography, astronomical observation, aerial survey, detection and high-resolution optical instruments. On the other hand, calcium fluoride single crystal doped with rare earth (RE) ions works well as an important solid laser gain medium, such as Yb:CaF_2 [3-5] and U:CaF_2 [6-10] single crystal.

However, it is well known that the manufacturing of single crystals has many disadvantages, including long fabrication period, the need for special devices, restricted size for products, as well as the segregation of RE ions resulting in the limit at high doping concentration. To overcome these problems, a new method, which has drawn considerable attention from the middle 1990s [11,12], arises to fabricate transparent ceramics, replacing single crystals by sintering RE ions doped nanopowders. Aubry et al. [13] reported the fabrication of Yb:CaF_2 transparent ceramics, using the corresponding nanopowders as raw materials. However, it has been demonstrated [14] that the properties of the starting nanopowders are the crucial factor which influences strongly on the properties of transparent ceram-

State Key Laboratory of Advanced Technology for Materials Synthesis and Processing, Wuhan University of Technology, Wuhan 430070, People's Republic of China
*Corresponding author. E-mail: zhigl1979@hotmail.com

ics. Thus, a number of synthesis methods were applied in the last several years: Li Yadong [15] synthesized RE:CaF_2 nanopowders with diameter of 100∼300 nm by hydrothermal method; Stark [16] prepared CaF_2 nanoparticles with diameter of 14 nm using flame synthesis, although the product yield was very low. In addition, Yb:CaF_2 [17] and Eu:CaF_2 [18] nanoparticles were also synthesized by wet chemical route in Igepal/cyclohexane/water reverse micelles system and polystyrene/THF solution, respectively.

Among the series of RE ions, the erbium element is the one interesting active ion having an intrinsic rich energy level, especially the up-conversion emission, and is believed to present high luminescence efficiency when incorporated into the low-phonon-energy CaF_2 matrix. The preparation of fine Er doped CaF_2 nanoparticles is expected to pave the way for the sintering of transparent ceramics, with potential applications in the fields such as lamps and display [19], the optical telecommunication [20], new optoelectronic devices [21] and biolabeling [22]. In this work, erbium doped CaF_2 nanopowders were synthesized by a microemulsion method in a CTAB/C_4H_9OH/C_7H_{16}/H_2O micelles system. Details on the absorption and emission spectra are discussed.

Experimental

The starting materials used in the experiments were $Ca(NO_3)_2{\cdot}4H_2O$(≥99.0%), NH_4F(≥96.0%), n-butyl alcohol(≥99.5%), n-heptane(≥97.0%), CTAB (Cetyltrimethyl Ammonium Bromide) (≥99.0%), $Er(NO_3)_3{\cdot}5H_2O$(≥99.9%), and ethanol(≥99.0%). The reagents were all provided by SCRC (Sinopharm Chemical Reagent Co., Ltd, China). De-ionized water was purified by the ultra-pure water system at our laboratory.

For the microemulsion experiment, a CTAB/C_4H_9OH /C_7H_{16}/H_2O system was used to synthesize the nanoparticles. Microemulsions were made by dissolving 11 g of CTAB in 27 ml of n-heptane inside a 100 ml teflon beaker. This mixture was stirred magnetically until it was homogeneous and clear. A 10 ml of 0.4 mol/l $Ca(NO_3)_2$ and $Er(NO_3)_3$ aqueous solution was poured in slowly and was stirred for a short time. Finally, a 14 ml of n-butyl alcohol, as a co-surfactant, was added into the solution. In a similar way, the microemulsions containing fluoride ions were made by substituting the calcium nitrate aqueous solution with 10 ml of 1.0 mol/l NH_4F aqueous solution. These two kinds of microemulsions were then mixed and stirred at room temperature for 30 min and the Er:CaF_2 nanoparticles generated according to the following reaction:Ca^{2+}+ Er^{3+}+ F^- → Er:CaF_2 ↓. The Er dopant concentrations were designed to be 0.2 mol%, 0.6 mol%, 1 mol%, 2 mol% and 6 mol%, respectively.

The emulsion mixture was centrifuged at a rate of 11000 rpm for 15 min, which caused sedimentation of the nanoparticles and allowed the removal of the mother liquor. The particles were then washed and centrifuged with ethanol and de-ionized water alternatively for several times. Finally the products were oven dried at 30℃ and lightly crushed in an agate mortar.

The direct precipitation method in aqueous solution was also applied for comparison with the microemulsion method. A solution containing the cationic precursors was made by dissolving nitrate salts in de-ionized water. Then this solution was added dropwise to the aqueous NH_4F solution which was stirred magnetically, leading to the formation of Er^{3+} doped CaF_2 nanoparticles. The separation and drying procedure were same as that described above.

X-ray diffraction (XRD) measurements were performed on D/Max-RB (Rigaku, Japan) using Cu Kα radiation. The 2θ angular resolution was 0.04°. The diffraction patterns were scanned slowly over the 2θ range 25∼60° at a rate of 2°/min.

Micromorphology of the obtained nanoparticles was observed by transmission electron microscopy (TEM, JEM-2100F, JEOL, Japan) and the samples were prepared on a holey carbon-coater copper TEM grid.

The IR spectra were obtained by using Fourier transform infrared spectroscopy (FTIR, Nexus, Thermo Nicolet, USA) to investigate the influence of annealing at different temperatures. The emission spectra were recorded on a fluorescence spectrophotometer (FP-6500, JASCO, Japan) equipped with a Xe-lamp as the excitation source. The excitation wavelength was 483 nm. All experiments were performed at room temperature.

Results and discussion

Figure 1 shows the XRD patterns of CaF_2 nanoparticles doped with trivalent erbium ions of 0.2 mol%, 0.6 mol%, 1 mol%, 2 mol% and 6 mol%, respectively, comparing with JCPDS standard card (35-0816) of the CaF_2 crystal. The patterns of samples exhibite peaks well in accordance with the standard card without other phase, indicating that the Er^{3+} doped CaF_2 nanoparticles were isostructural with CaF_2 crystal. The full width at half maximum (FWHM) of peaks shows a broadening trend with the doping concentration, which indicates the incorporation of Er^{3+} facilitated the decrease in grain size and crystallinity. The XRD results also show the shifts in diffraction angles. This is the consequence of the incorporation of foreign ions into the lattice structure of host materials resulting in the changes of lattice parameters.

Figure 2 shows the TEM images of 0.2 mol% Er^{3+}

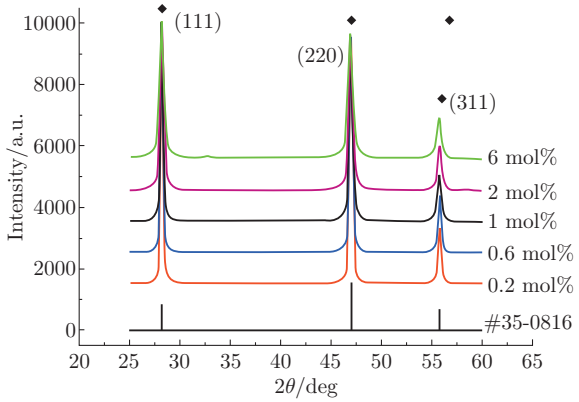

Fig. 1 XRD patterns of CaF_2 nanoparticles doped with Er^{3+} at different concentration.

doped CaF_2 nanoparticles synthesized by the microemulsion method and direct precipitation method. The particles of CaF_2 with no agglomeration prepared by microemulsion were uniform in grain size of about 20 nm (see Fig. 2(a)). The nanoparticles with the same chemical composition prepared by aqueous solutions direct precipitation method was un-homogenous in grain size and severely agglomerated as presented in Fig. 2(b). The reaction by the micromulsions method took place inside the micro-micelles in which there were limited amounts of reaction reagents, namely, this method could control the grain growth in these microreactors. In the process of direct precipitation, conversely, the instantaneous local concentrations differed greatly when being mixed, resulting in the different numbers of nucleation and grain growth rate.

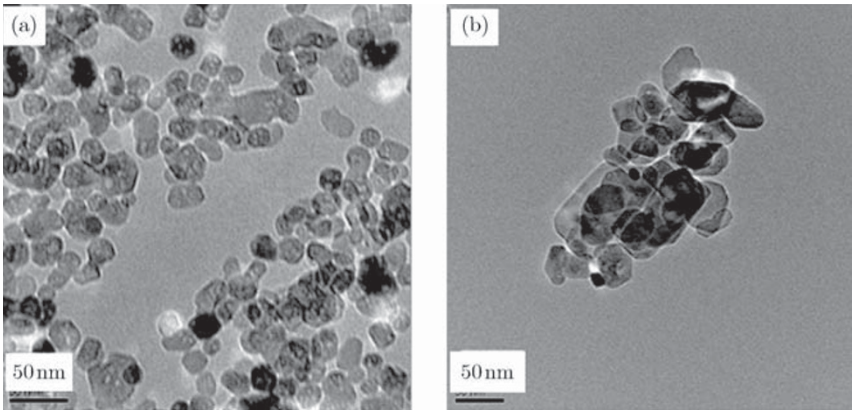

Fig. 2 TEM images of CaF_2 nanoparticles synthesized by reverse microemulsion (a) and direct precipitation (b).

The IR absorption spectra were used to determine whether the surfactants and nitrates were removed completely from the product prepared by reverse microemulsion after washing. As shown in Fig. 3, the sharp peaks at 2856 cm^{-1} and 2928 cm^{-1} are assigned to the symmetric and antisymmetric stretching vibration of the -CH_2 groups. The broad peaks at 3453 cm^{-1} and 1635 cm^{-1} are assigned to the symmetrically stretching vibration and asymmetric stretching vibration of -OH, implying the presence of H_2O molecules. The peak at 1385 cm^{-1} is the asymmetric stretching vibration of NO_3^-. Residual organics were also detected on the spectrum of the as synthesized powder around 1093 cm^{-1}. FTIR analysis shows that inorganic groups were not removed completely by the washing procedure; some of them are adsorbed on the surfaces of the particles due to the high surface energy originating from large surface area. Besides, as can be seen in Fig. 3, the FTIR spectra recorded on the synthesized powder after annealing at different temperatures are also presented. After annealing at 400℃, the traces of organics were removed and the amounts of nitrates were strongly decreased. With the increase in the annealing temperatures from 400℃ to 600℃, the nitrates could not be detected any more. The intensity of the strong absorption bands related to the presence of water or hydroxyl groups in the as obtained powder decrease continuously with the increase in annealing temperature revealing a decrease in the amount of these molecules or groups.

The absorption spectra of CaF_2 powders with dif-

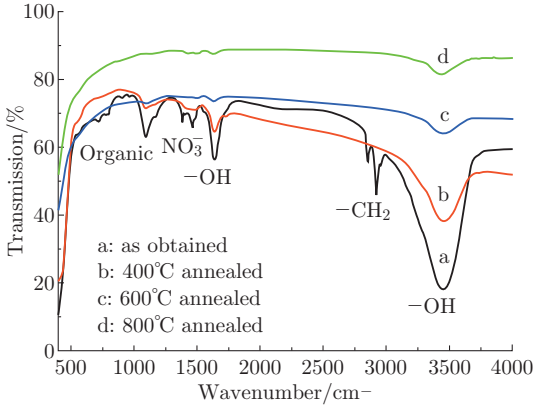

Fig. 3 FTIR spectra of Er^{3+}:CaF_2 nanoparticles annealed at different temperature.

ferent Er^{3+} dopant annealed at 400℃ are shown in Fig. 4. The effect of annealing on the characteristic absorption peaks of trivalent erbium ion is not obvious, in contrast with intensive absorption peaks attributed to the existense of -OH, $-CH_2$, NO_3^- and organic groups in the range of IR as shown in Fig. 3. Experimental results indicate that there are many absorption bands and the absorption intensity increases with the dopant concentration. The band in the ultraviolet region between 340 and 380 nm with a maximum around 374 nm can be assigned to the $^4I_{15/2} \rightarrow ^4G_{11/2}$ transition. The two bands between 390 and 500 nm with maximum around 402 and 480 nm can be assigned to $^4F_{7/2} \rightarrow ^2H_{9/2}$ and $^4I_{15/2} \rightarrow ^4F_{7/2}$transitions. The remaining bands centered at 515, 648, 788 and 960 nm, as well as the broad absorption band around 1500 nm correspond to the following transitions of Er^{3+}, $^4I_{15/2} \rightarrow ^2H_{11/2}$, $^4I_{15/2} \rightarrow ^4F_{9/2}$, $^4I_{13/2} \rightarrow ^2H_{11/2}$, $^4I_{15/2} \rightarrow ^4H_{11/2}$ and $^4I_{15/2} \rightarrow ^4I_{13/2}$, respectively. Furthermore, the absorption peak and band corresponding to the $^4I_{15/2} \rightarrow ^4H_{11/2}$ and $^4I_{15/2} \rightarrow ^4I_{13/2}$ transitions show somewhat a shift to IR, especially for the latter. This can be regarded as a consequence of weakened energy level split. It is well known that, in Er^{3+} doped CaF_2 crystals, the cluster structures would appear when the doping concentration is higher than 0.05 at ·% [23] and the ions in clusters dominate when the doping concentration is higher than 0.2 at ·%, resulting in that the influences of crystal field of host is weakened strongly with the increase in doping concentration. Therefore the energy level splits of active ions are also weakened. However, shifts of other absorption peaks are not found or too weak to be observed. It may be inferred that the changes of crystal field strength would influence the high energy levels slightly more, relative to the low energy levels.

The annealing process has a strong influence on the emission spectra of Er^{3+} doped CaF_2 nanopowders.

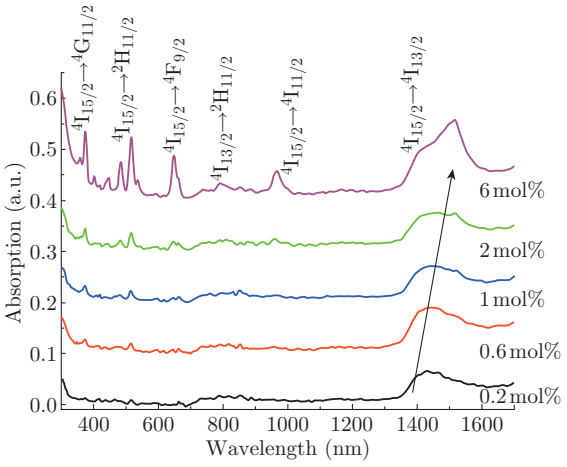

Fig. 4 Absorption spectrum of Er^{3+}:CaF_2 nanopowders with different dopant concentration.

The contrast of emission spectra of annealed powder at 400℃ and un-annealed powder doped with 6 mol% Er^{3+} is shown in Fig. 5. The wavelength of excitation light was 483 nm. It can be seen from Fig. 5 that the emission intensity of the sample annealed at 400℃ is stronger than that of the as-obtained nanoparticles, especially at the wavelength bands in the 525∼570 nm region. The peaks centered at 540 nm and 546 nm can be attributed to the energy transfer $^4S_{3/2} \rightarrow ^4I_{15/2}$, while the peaks centered at 552 nm and 558 nm can be assigned to the energy transfer $^2G_{9/2} \rightarrow ^4I_{13/2}$. The broad bands are caused by the energy level split of $^4I_{15/2}$ and $^4I_{13/2}$ ground state. The relatively weaker emission intensity of as-obtained nanoparticles can be generally attributed to size and surface effects. It is known that the coordination of atoms on the surface is different from that in the bulk; atoms on the surface do not have a full coordination sphere which leads to a higher potential energy. Therefore, various chemical species can easily be adsorbed on the surfaces of the particles. Considering that our synthesis process was achieved with nitrate salt in water, the surface of the nanoparticles could be covered by residual NO_3^- and OH^- groups, as detected by FTIR spectroscopy. Such groups, with high phonon frequencies, are well known to quench efficiently the luminescence and resulted in the weak emission intensity of the as-obtained nanoparticles. Once they were heated up to 400℃, the treatment would remove the species adsorbed on the surfaces of the particles through their desorption and decomposition during the annealing process, resulting in the decrease in the amount of quenching centers; thus, the luminescence efficiency would improve and the decay time increased strongly.

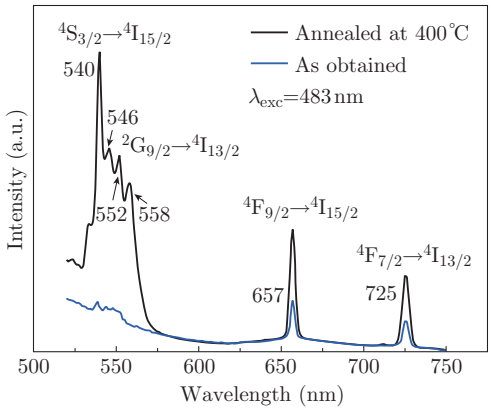

Fig. 5 Emission spectrum of Er^{3+}:CaF_2 nanopowders with different dopant concentration.

Figure 6 shows the Er^{3+} dopant concentration dependence of the emission of Er^{3+}:CaF_2 nanopowders annealed at 400℃ by monitoring the $^4F_{7/2} \rightarrow ^4I_{13/2}$ transition centered at 725 nm. The excitation wavelength was 483 nm. These five spectra presented similar shape. It can be seen in Fig. 6 that with the increase

of dopant concentration from 0.2 to 6.0 mol%, the intensity of spectra did not show distinct enhancement as that of the absorption spectra. This observation could be related to the grain nano-scale size, as well as the cluster structure in the host CaF_2, leading to concentration quenching. Moreover, it is easy to evaluate that the fluorescence wavelength reveal a Blue-Shift with the doping amounts of Er^{3+}. This can also be attributed to the weak of energy level spilt mentioned above.

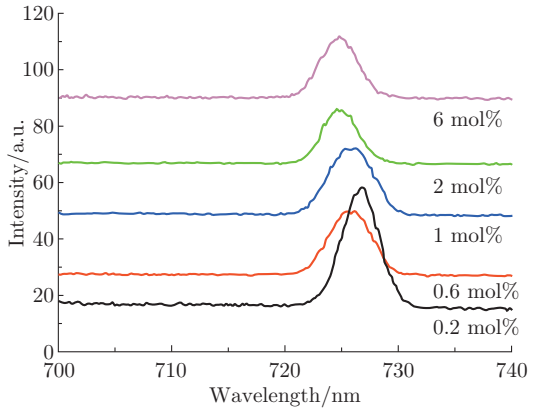

Fig. 6 Er^{3+} dopant concentration dependence of the emission of Er^{3+}:CaF_2 nanopowders annealed at 400℃.

Conclusions

CaF_2 nanopartiles doped with different amounts of erbium have been synthesized by the microemulsion method. The as-obtained particles, compared with those synthesized by direct precipitation methods, presented uniform morphology with mean grain size of about 20 nm. The incorporation of Er^{3+} into the CaF_2 facilitates the decrease in grain size and changes of lattice parameter. The FTIR spectra indicate that there are still some amounts of NO_3^-, -OH or water molecules and organic groups adhering to the particle surfaces. The absorption spectra show that the absorption intensity increases with the doping concentration. Red-Shift of absorption spectra and Blue-Shift of emission spectra can be attributed to the decrease in the field strength of the CaF_2 host. Annealing has a profound effect on the emission spectra. The emission intensity does not show an increasing trend with the increasing amount of Er^{3+} dopant, but reveal a Blue-Shift of the emission peak at 725 nm.

Acknowledgment

The project is funded by the National Natural Science Foundation of China (NO. 51072144) and State Key Laboratory of Advanced Technology for Materials Synthesis and Processing (Wuhan University of Technology) (NO. 2009-ZT-1)

References

[1] J. Tu, S. A. Fitgerald, J. A. Campbell and A. J. Sievers, J. Non-cryst. Solids 203, 153(1996). http://dx.doi.org/10.1016/0022-3093(96)00346-8

[2] L. Dressler, R. Rauch and R. Reimann, Cryst. Res. Technol. 23, 413 (1992). http://dx.doi.org/10.1002/crat.2170270320

[3] V. Petit, J. L. Doualan and P. Camy, Appl. Phys. B 78, 681 (2004). http://dx.doi.org/10.1007/s00340-004-1514-6

[4] A. Lucca, M. Jacquemet and F. Druon, Opt. Lett. 29, 1879 (2004). http://dx.doi.org/10.1364/OL.29.001879

[5] A. Lucca, G. Deboug, M. Jacquemet and F. Druon, Opt. Lett. 29, 2767 (2004). http://dx.doi.org/10.1364/OL.29.002767

[6] P. P. Sorokin and M. J. Stevenson, Phys. Rev. Lett. 5, 557 (1960). http://dx.doi.org/10.1103/PhysRevLett.5.557

[7] G. D. Boyd, R. J. Collins, S. P. S. Porto, A. Y. Excitation and W. A. Hargreaves, Phy. Rev. Lett. 8, 269 (1962). http://dx.doi.org/10.1103/PhysRevLett.8.269

[8] L. B. Su, J. Xu, Y. J. Dong, W. Q. Yang, G. Q. Zhao and G. J. Zhao, J. Cryst. Growth 261, 496 (2004). http://dx.doi.org/10.1016/j.jcrysgro.2003.09.036

[9] L. B. Su, W. Q. Yang, J. Xu, Y. J. Dong and G. Q. Zhao, J. Cryst. Growth 270, 150 (2004). http://dx.doi.org/10.1016/j.jcrysgro.2004.06.013

[10] L. B. Su, W. Q. Yang, J. Xu, Y. J. Dong and G. Q. Zhao, J. Cryst. Growth 273, 234 (2004). http://dx.doi.org/10.1016/j.jcrysgro.2004.08.028

[11] A. Ikesue, I. Furusato and K. Kamata, J. Am. Ceram. Soc. 78, 225 (1995). http://dx.doi.org/10.1111/j.1151-2916.1995.tb08389.x

[12] A. Ikesue, T. Kinoshita, K. Kamata and K. Yoshida, J. Am. Ceram. Soc. 78, 1033 (1995). http://dx.doi.org/10.1111/j.1151-2916.1995.tb08433.x

[13] P. Aubry, A. Bensalah, P. Gredin, G. Patriarche, D. Vivien and M. Mortier, Opt. Mater. 31, 750 (2009). http://dx.doi.org/10.1016/j.optmat.2008.03.022

[14] K. V. Dukel'skii, I. A. Mironov, V. A. Demidenko and A. N. Smirnov, J. Opt. Technol. 75, 728 (2008).

[15] X. M. Sun and Y. D. Li, Chem. Commun. 14, 1768 (2003). http://dx.doi.org/10.1039/b303614f

[16] R. N. Grass and W. J. Stark, Chem. Commun. 13, 1767 (2005). http://dx.doi.org/10.1039/b419099h

[17] A. Bensalah, M. Mortier, G. Patriarche, P. Gredin and D. Vivien, J. Solid State Chem. 179, 2636 (2006). http://dx.doi.org/10.1016/j.jssc.2006.05.011

[18] F. Wang, X. P. Fan, D. B. Pi and M. Q. Wang, Solid State Commun. 133, 775 (2005). http://dx.doi.org/10.1016/j.ssc.2005.01.014

[19] T. Jüstel, H. Nikol and C. Ronda, Angew Chem. Int. Edit. 37, 3084 (1998). http://dx.doi.org/10.1002/(SICI)1521-3773(19981204)37:22$<$3084::AID-ANIE3084$>$3.0.CO;2-W

[20] D. B. Barber, C. R. Pollock, L. L. Beecroft and C. K. Ober, Opt. Lett. 22, 1247 (1997). http://dx.doi.org/10.1364/OL.22.001247

[21] K. Kawano, K. Arai, H. Yamada, N. Hashimoto and R. Nakata, Sol. Energy Mater. Sol. Cells 48, 35 (1997). http://dx.doi.org/10.1016/S0927-0248(97)00066-4

[22] M. Wang, C. C. Mi, J. L. Liu, X. L. Wu, Y. X. Zhang, W. Hou, F. Li and S. K. Xu, J. Alloy. Compd. 485, 24 (2009). http://dx.doi.org/10.1016/j.jallcom.2009.05.138

[23] D. R. Tallant and J. C. Wright, J. Chem. Phys. 63, 2074 (1975). http://dx.doi.org/10.1063/1.431545